required. Unlike excited-state photon echoes which tend to become weaker as the oscillator strength of the excited transition decreases,[11] tri-level echoes should remain of constant intensity as long as the lasers can produce 180° pulses for the transitions involved. Reference 11 shows how modest these power requirements are, and it is thus reasonable to believe that tri-level echoes will be observable when state $|2\rangle$ is a highly excited state in virtually any element. Tri-level echoes should thus be an extremely powerful tool for relaxation studies in both pulsed and cw experiments. Finally, we mention one surprising observation: Under the conditions described in the paragraph preceding Eq. (1), with $t_1=t_2=0$, an undelayed signal at $\omega=\omega_1$ occurs at $t=t_3$ when state $|2\rangle$ is the $5^2S_{1/2}$ state and $\hat{k}_1\cdot\hat{k}_2 = -1$. In this case no echo should appear according to the analysis following Eq. (1), since $\omega_2 < \omega_1$ and hence $t_4 < t_3$. The "echo" we see is not fully understood at present, but we believe that this apparent "echo" may actually be free-induction decay of the ensemble-average $|0\rangle - |1\rangle$ superposition which is created at t_3 as if it were coherent shortly before at $t_4 < t_3$.

This work was supported by the Joint Services Electronics Program (U. S. Army, U. S. Navy, U. S. Air Force) under Contract No. DAAG29-77-C-0019.

[1]E. L. Hahn, Phys. Rev. 80, 580 (1950).
[2]I. D. Abella, N. A. Kurnit, and S. R. Hartmann, Phys. Rev. 141, 391 (1966).
[3]P. Hu, S. Geschwind, and T. M. Jedju, Phys. Rev. Lett. 37, 1357, 1773(E) (1976).
[4]S. R. Hartmann, IEEE J. Quant. Electron. 4, 802 (1968).
[5]The nature of tri-level echoes in a solid in which inhomogeneous broadening is due to variations of local perturbing fields is determined by the precise way in which each of the three states is shifted with respect to the others.
[6]M. Aihara and H. Inaba, Opt. Commun. 8, 280 (1973), and J. Phys. A 6, 1709, 1725 (1973).
[7]Hiroshi Hatanaka, Takehiko Terao, and Tsuneo Hashi, J. Phys. Soc. Jpn. Lett. 39, 835 (1975).
[8]If $t_1=t_2$, echoes should also occur if ω_1 and ω_2 satisfy the weaker condition $\omega_1+\omega_2=\Omega_{20}$. In this case ω_3 must still be resonant with Ω_{21}.
[9]M. Scully, M. J. Stephen, and D. C. Burnham, Phys. Rev. 171, 213 (1968).
[10]The normal two-pulse photon echo occurring in an ensemble of two-level systems is conventionally described as arising from the reversal of phase of each atomic superposition by the second pulse. In our notation, this manifests itself by $\varphi = 2\vec{k}_2\cdot\vec{x}_2 - \vec{k}_1\cdot\vec{x}_1$, where now $|\vec{k}_2| = |\vec{k}_1| = \Omega_{10}/c$, but $\vec{x}_2$ and $\vec{x}_1$ are given as before. For an analysis of the radiated field see Ref. 9.
[11]A. Flusberg, T. Mossberg, and S. R. Hartmann, to be published.
[12]P. F. Liao, N. P. Economou, and R. R. Freeman, Phys. Rev. Lett. 39, 1473 (1977).
[13]F. Biraben, B. Cagnac, E. Giacobino, and G. Grynberg, J. Phys. B 10, 2369 (1977); G. Grynberg, private communication.

Direct Measurement of Compression of Laser-Imploded Targets Using X-Ray Spectroscopy

B. Yaakobi, D. Steel,[a] E. Thorsos, A. Hauer, and B. Perry
Laboratory for Laser Energetics, University of Rochester, Rochester, New York 14627
(Received 28 September 1977)

Compression of neon-filled glass microballoons irradiated by a four-beam laser system has been measured directly by Stark broadening, opacity broadening, and spatial profiles of Ne^{+9} x-ray lines. For an 8.6-atm fill pressure and a 0.2-TW, 40-psec laser pulse, the measured compressed neon density was 0.26 g/cm^3 and the product ρR was 2.5×10^{-4} g/cm^2.

The most important parameter in laser-induced fusion experiments, namely the product, ρR, of compressed core density and radius, has been inferred from the dimensions of the region emitting x rays or α particles.[1,2] In this Letter it is shown that spectral profiles of neon x-ray lines from neon-filled targets yield *direct* information on both ρ and ρR. This measurement does not require one to assume that the hot core contains the whole mass of the fill gas; nor does the problem exist of raising an uncertain core radius to the third power. The targets in these experiments were filled with neon only, at either 2.0- or 8.6-atm pressure. However, the same diagnostic methods can apply to a mixture of neon and a thermonuclear fuel; spectra like these obtained here can be expected with only a small amount of neon in future high-ρR experiments.

The experiments were performed on the DELTA four-beam laser system producing power on tar-

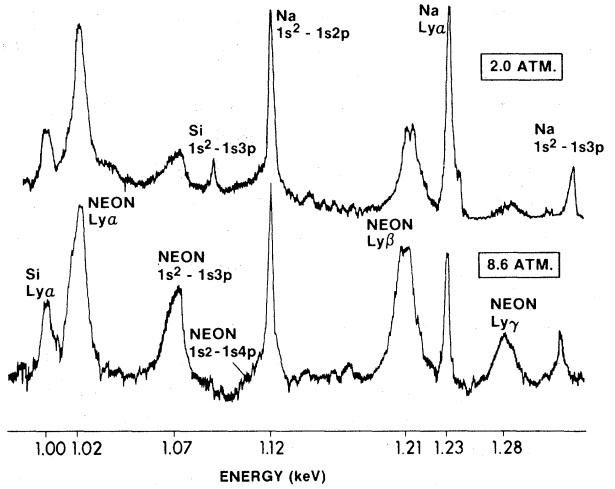

FIG. 1. Microdensitometer traces (in same scale) of the x-ray spectrum from imploded neon-filled glass microballoons at two different fill pressures. ρR increases with fill pressure.

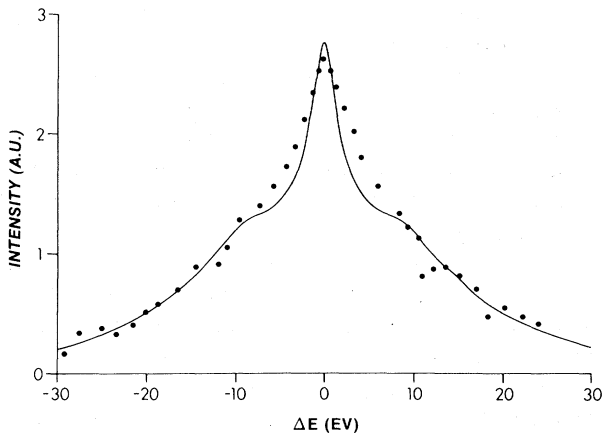

FIG. 2. Compression measurement: fitting a Stark profile of $N_e = 7 \times 10^{22}$ cm^{-3} to the experimental profile of the Lyman-γ line of neon (9.7 Å).

get of 0.15–0.2 TW in pulses of 40 psec full width at half-maximum (FWHM). Neon x-ray line spectra were obtained consistently on single-shot exposures (optical density $\lesssim 0.3$) and no significant changes were observed for power variations in this range. A thalium acid phthalate crystal spectrograph equipped with a slit of width 11 μm was used, giving simultaneously spatially integrated spectra and spatially resolved spectra of resolution 13 μm (at 10 Å). Typical target diameter was 65 μm with a nominal wall thickness 0.6 μm.

Figure 1 shows part of the x-ray spectrum emitted from glass microballoons filled with neon at 2.0- and 8.6-atm pressure. The Ne^{+8} and Ne^{+9} x-ray lines are seen to be considerably broader than the sodium lines from the glass shell. Their width (FWHM as large as 20 eV) is much larger than the width (~ 1.5 eV) due to crystal inperfection and finite size of the source. As we go from 2.0- to 8.6-atm fill pressure the intensity of neon lines increases by varying amounts. For example, the intensity of the Lyman-α line remains nearly constant as the fill pressure increases. This is clear evidence of saturation due to the self-absorption (or opacity) of this line. As higher series members are progressively less self-absorbed, the Lyman-β line approaches the blackbody limit for the 8.6-atm case. However, the Lyman-γ line remains optically thin: Although it increases substantially with fill pressure it is still much below the blackbody limit indicated by the other lines. In terms of the optical depth at line center (τ_0) we have then $\tau_0(\mathrm{Ly}\alpha) \gg 1$, $\tau_0(\mathrm{Ly}\beta) \sim 1$, and $\tau_0(\mathrm{Ly}\gamma) \ll 1$. The results below turn out to be entirely consistent with these results. Moving to higher series members the broadening due to opacity decreases rapidly whereas Stark broadening increases (other broadening mechanisms are negligible).[3] The spectrum therefore yields two kinds of complementary measurements: The Stark profile of the Lyman-γ line gives the density (hence the compression) and the opacity-broadened Lyman-α line gives the ρR product.

Figure 2 shows a comparison of the best-fit calculated Stark profile with the measured Lyman-γ line for the 8.6-atm case. Doppler and instrumental profiles were folded into the calculated profiles but they only have a small effect. The Stark profiles have been calculated by Hooper and Tighe[4] for the case of Ne^{+9} lines perturbed by a Ne^{+9} ion plasma. The electron temperature T_e during the emission of neon lines needs only to be known approximately for these calculations. Using the measured intensity ratio $I(1s\text{-}3p)/I(1s^2\text{-}1s3p)$ we estimate T_e to be ~ 300 eV. The intensity ratio between Lyα and Lyβ corresponds to a Planck distribution of about the same T. Figure 2 shows that the electron density for the 8.6-atm case is 7×10^{22} cm^{-3} which corresponds to a mass density 0.26 g/cm^3. The uncertainty in N_e was found to be $\pm 25\%$ by varying the temperature and the assumed background level within their estimated error brackets. Assuming that the whole neon mass is uniformly compressed we derive a diameter $D = 19$ μm for the compressed neon core and a ρR value of 2.5×10^{-4} g/cm^2 (here R is the average chord length, $2D/\pi$). The compression ratio is 38. For the 2.0-atm case the final den-

sity is approximately the same and the compression ratio is ~ 150.

We next analyze the optically thick Lyman-α line profile which is shown in Fig. 3 for the two pressure cases. Under the assumption of a homogeneous source, the line radiative transport equation can be solved and gives (in local thermodynamic equilibrium) $I_\nu = B_\nu{}^T[1 - \exp(-\tau_0 P_\nu/P_0)]$, where I_ν is the observed line profile at frequency ν, $B_\nu{}^T$ is Planck's function (blackbody limit) for a temperature T, P_ν is the intrinsic line profile, and τ_0 the optical depth at line center (or at frequency at which P_0 is evaluated). If $\tau_0 \gg 1$, I_ν has a flat top of intensity $B_\nu{}^T$ and is wider than the source (i. e., Stark) width. This is what is indicated by Fig. 3 where the measured Lyman-α profile is wider than the Stark width calculated for the density found from the Lyman-γ line. Fitting I_ν profiles to the observed profile for the 8. 6-atm case, we find $\tau_0/P_0 = 2\times10^{16}$ sec^{-1}, using the Stark profile for $N_e = 7\times10^{22}$ cm^{-3}. The optical depth is related to ρR through $\rho R = (\tau_0/P_0)(mMc/\pi e^2 f)b^{-1}$ where M is the ion mass, f is the line oscillator strength, and b is the fraction of all neon ions which are in the ground state of Ne^{+9}. Over a wide temperature range in which Ne^{+9} emission is significant[3] $b \sim 0.3$ which gives $\rho R = 2.2\times10^{-4}$ g/cm^2. This value agrees well with that obtained above. The optical depth at the peak of the (electron-broadened) unshifted Stark component is ~ 100. For the 2-atm pressure case, $\rho R \sim 1\times10^{-4}$ g/cm^2.

We finally fit Stark profiles to the Lyman-β line. Figure 4(a) shows the best fit for the 2-atm pressure case which yields the same density value as obtained from the Lyman-γ line: $N_e \sim 7\times10^{22}$ cm^{-3}. For the 8.6-atm case [Fig. 4(b)] the same profile has the wrong width and shape. However, fitting a profile from a uniform source with the same density but an optical depth at line center $\tau_0 = 0.5$ (or $\tau = 1.2$ at the peaks) we get good agreement with the experimental profile. To check consistency we calculate τ_0(Lyβ) using the ρR values obtained from the Lyman-α line. We get for the 2-atm case $\tau_0 \sim 0.4$ and for the 8.6-atm case $\tau_0 \sim 0.8$ (for the peaks of the profile $\tau \sim 2.5\tau_0$).

We finally consider spatial profiles of neon lines. As an example, Fig. 5 shows the spatial profile of the neon Lyman-β line for the 8. 6-atm case. The diameter of the compressed neon core (especially after subtracting the continuum) is seen to agree very well with the value (19 μm) inferred from the spectral profiles.

In conclusion, Stark broadening, opacity broadening, and spatial profiles of neon x-ray lines all give consistent, direct measurements of both the compressed density and ρR of a laser-imploded

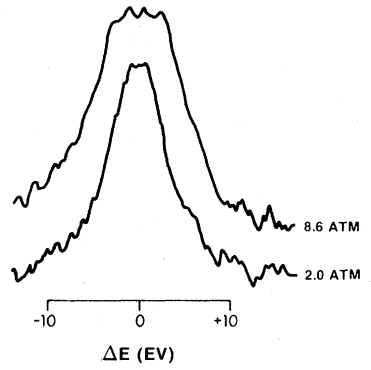

FIG. 3. ρR measurement: opacity-broadened Lyman-α line of neon (12.13 Å) for two filling pressures. The FWHM is 7.5 and 12 eV whereas the Stark width as inferred from Fig. 2 is 5.5 eV (ion broadening only).

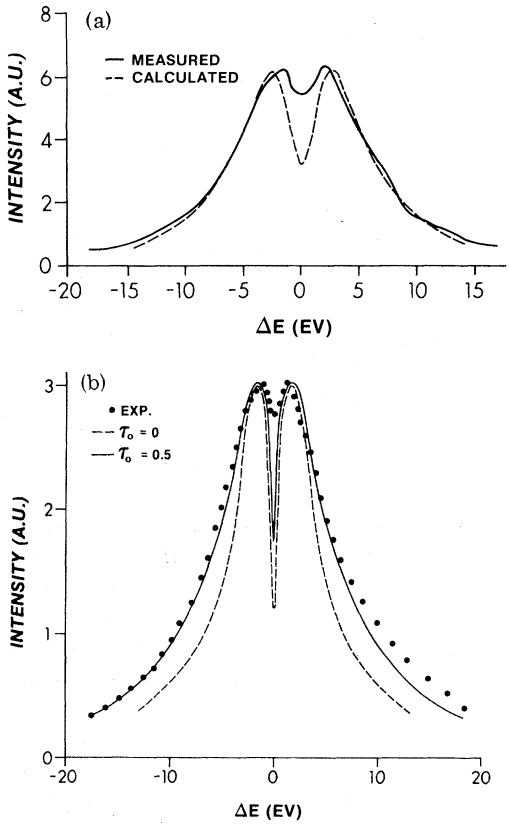

FIG. 4. Compression measurements: Fitting of a Stark profile of $N_e = 7\times10^{22}$ cm^{-3} to the experimental profile of the Lyman-β line of neon (10.24 Å) at (a) 2 atm fill pressure and (b) at 8.6 atm fill pressure. τ_0 is the assumed optical depth at line center.

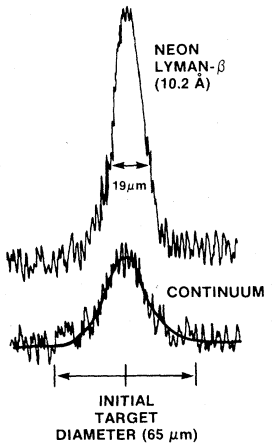

FIG. 5. Spatial profile of the Lyman-β line of neon (10.24 Å), and the nearby continuum. The bar indicates the compressed neon diameter as inferred from spectral profiles analysis.

target. Neon doping in future laser fusion targets may be interesting not only as a diagnostic probe but also as a means of controlling the implosion dynamics.[5] At low enough impurity content the dominant effect would be the inhibition of heat loss from the fuel to the tamper; at higher impurity content the dominant effect would be the cooling of the fuel by radiation losses, thereby enabling a higher compression.

The contribution of the following persons was indispensable to the success of this work: J. Geiger, A. Nee, J. Halpern, H. Deckman, E. Lazarus, J. Grosso, C. F. Hooper, and L. M. Goldman.

[a]On assignment from Exxon Research and Engineering Company.

[1]P. M. Campbell, G. Charatis, and G. R. Montry, Phys. Rev. Lett. 34, 74 (1975).

[2]N. M. Ceglio and L. W. Coleman, Phys. Rev. Lett. 39, 20 (1977).

[3]H. R. Griem, *Plasma Spectroscopy* (McGraw-Hill, New York, 1964), and *Spectral Line Broadening* (Academic, New York, 1974).

[4]C. F. Hooper, Jr., private communication; also, R. J. Tighe, dissertation, University of Florida (unpublished); R. J. Tighe and C. F. Hooper, Phys. Rev. A 15, 1773 (1977). A full description of these profile calculations is being prepared for publication by C. F. Hooper.

[5]S. L. Bogolyubskii *et al.*, Pis'ma Zh. Eksp. Teor. Fiz. 24, 206 (1976) [JETP Lett. 24, 182 (1976)].

Brillouin Scatter in Laser-Produced Plasmas

D. W. Phillion, W. L. Kruer, and V. C. Rupert
Lawrence Livermore Laboratory, University of California, Livermore, California 94550
(Received 29 July 1977)

The absorption of intense laser light is found to be reduced when targets are irradiated by 1.06-μm light with long pulse widths (150–400 ps) and large focal spots (100–250 μm). Estimates of Brillouin scatter which account for the finite heat capacity of the underdense plasma predict this reduction. Spectra of the back-reflected light show red shifts indicative of Brillouin scattering.

In laser fusion applications it is important to understand the absorption of laser light when the product of intensity and the square of the wavelength exceeds $\sim 10^{15}$ W μm^2/cm^2. In such experiments,[1-7] it was generally found that Brillouin scatter[8-10] is limited at a low level, an effect which has been attributed theoretically[9,10] to the small mass and heat capacity of the small underdense plasma. With the advent of more powerful lasers, it is becoming common to investigate the absorption of intense light in experiments with long pulses and large focal spots. These experiments, characterized by a much larger region of underdense plasma, more closely approximate future experiments with shaped pulses. For example, a simple estimate shows that the size of the underdense plasma $L \approx R$, where R is the radius of the focal spot, provided that the pulse length is long enough for plasma to expand that far.

With large regions of underdense plasma, stimulated scattering of the incident laser light becomes a concern. First we briefly present a simple estimate for Brillouin scattering, which takes into account the finite heat capacity of the underdense plasma. Although crude, this model suffices to estimate magnitudes and also to emphasize the strong ion heating concomitant with the